Check for updates

Geophysical Research Letters

RESEARCH LETTER
10.1029/2022GL100270

Key Points:

- Northern Hemisphere land monsoon precipitation has significantly decreased over the past 120 years
- Anthropogenic aerosol has a more significant contribution to precipitation reduction than greenhouse gases
- Surface radiation and monsoon circulation dominate the aerosol's high efficiency in reducing monsoon precipitation

Supporting Information:

Supporting Information may be found in the online version of this article.

Correspondence to:

J. Cao and B. Wang,
jianc@nuist.edu.cn;
wangbin@hawaii.edu

Citation:

Cao, J., Wang, H., Wang, B., Zhao, H., Wang, C., & Zhu, X. (2022). Higher sensitivity of Northern Hemisphere monsoon to anthropogenic aerosol than greenhouse gases. *Geophysical Research Letters*, *49*, e2022GL100270. https://doi.org/10.1029/2022GL100270

Received 2 JUL 2022
Accepted 5 OCT 2022

Author Contributions:

Conceptualization: Jian Cao, Bin Wang
Formal analysis: Jian Cao, Hao Wang
Methodology: Jian Cao
Supervision: Bin Wang
Writing – original draft: Jian Cao
Writing – review & editing: Jian Cao, Bin Wang, Haikun Zhao, Chao Wang, Xiaowei Zhu

© 2022. American Geophysical Union. All Rights Reserved.

Higher Sensitivity of Northern Hemisphere Monsoon to Anthropogenic Aerosol Than Greenhouse Gases

Jian Cao[1,2], Hao Wang[1], Bin Wang[2,3], Haikun Zhao[1], Chao Wang[1], and Xiaowei Zhu[4]

[1]Key Laboratory of Meteorological Disaster, Ministry of Education/Joint International Research Laboratory of Climate and Environment Change/Collaborative Innovation Center on Forecast and Evaluation of Meteorological Disasters, Nanjing University of Information Science and Technology, Nanjing, China, [2]Earth System Modeling Center, Nanjing University of Information Science and Technology, Nanjing, China, [3]Department of Atmospheric Sciences, University of Hawaii at Mānoa, Honolulu, HI, USA, [4]Ningxia Climate Center, Ningxia, China

Abstract Because increased greenhouse gas emissions considerably warm and moisten the Earth's atmosphere, one may expect an increase in monsoon precipitation during the historical period. However, we find the observed Northern Hemisphere land summer monsoon (NHLM) precipitation has significantly decreased since 1901. Simulations from Coupled Model Intercomparison Project Phase 6 (CMIP6) well reproduce global warming and the drying of NHLM since the industrial revolution when forced by observed external forcings. Result from single forcing experiment shows that the anthropogenic aerosol (AA) dominates the Northern Hemisphere (NH) monsoon precipitation drying, while the greenhouse gases (GHG) largely control surface warming. Thus, the NH monsoon precipitation responds to AA more sensitively than the GHG. The AA can more effectively modulate downward solar radiation reaching the surface, decreasing evaporation and weakening monsoon circulations by reducing the interhemispheric temperature difference and land-ocean thermal contrast, albeit with the same efficiency of the thermodynamic effect in the two forcings. Our result indicates the future intensive reduction of aerosol emission may rapidly recover the NH monsoon precipitation.

Plain Language Summary Increased anthropogenic emissions from human activities significantly warm the Earth system. In common sense, it would increase monsoon precipitation. However, observed Northern Hemisphere (NH) monsoon precipitation shows a significant decline since the beginning of the 20th century. The current state-of-the-art models reproduce the global warming and weakened NH monsoon under anthropogenic aerosol (AA) and greenhouse gases (GHG) forcing. We find that AA dominates the monsoon precipitation change but only has a minor role in the Earth's surface temperature. In contrast, the GHG controls the Earth's surface warming but has a minor role in changing monsoon precipitation. It suggests that the aerosols are more effective in changing NH monsoon precipitation than GHG. Our result indicates the future intensive reduction of aerosol emission may rapidly increase the NH monsoon precipitation under global warming.

1. Introduction

Change in Northern Hemisphere (NH) monsoon precipitation affects the water resource availability for two-thirds of the world's population. In common sense, global warming would increase monsoon precipitation. Studies show that the NH monsoon precipitation increases under future global warming (e.g., Cao et al., 2020; Cao & Zhao, 2020; Chadwick et al., 2013; Kitoh et al., 2013; Lee & Wang, 2014; Moon & Ha, 2020; Wang et al., 2020). The increase in global mean surface temperature (GMST) enhances atmospheric moisture, contributing to the increased precipitation (Jin et al., 2020; Kitoh et al., 2013; Monerie et al., 2022). On the other hand, the weakening of tropical circulation due to the increased atmospheric static stability partially cancels the thermodynamic effect, resulting in a moderate increase in NH monsoon precipitation (Cao et al., 2019; Chadwick et al., 2013; Hsu et al., 2013; Kitoh et al., 2013; Wang et al., 2020).

However, it is not the case for historical NH monsoon precipitation and GMST change. The observed NH land summer monsoon (NHLM) precipitation is decreased under historical global warming, especially since the 1950s (Figure 1, Figure S1 in Supporting Information S1, monsoon domain as in Figure S2 in Supporting Information S1) (Herman et al., 2020; Polson et al., 2014; Vicente-Serrano et al., 2021; Wang & Ding, 2006; Zhang & Zhou, 2011; Zhou et al., 2008, 2020). Although anthropogenic aerosol (AA) and greenhouse gas (GHG) can both

19448007, 2022, 20, Downloaded from https://agupubs.onlinelibrary.wiley.com/doi/10.1029/2022GL100270 by CochraneChina, Wiley Online Library on [22/10/2022]. See the Terms and Conditions (https://onlinelibrary.wiley.com/terms-and-conditions) on Wiley Online Library for rules of use; OA articles are governed by the applicable Creative Commons License

19448007, 2022, 20, Downloaded from https://agupubs.onlinelibrary.wiley.com/doi/10.1029/2022GL100270 by CochraneChina, Wiley Online Library on [22/10/2022]. See the Terms and Conditions (https://onlinelibrary.wiley.com/terms-and-conditions) on Wiley Online Library for rules of use; OA articles are governed by the applicable Creative Commons License

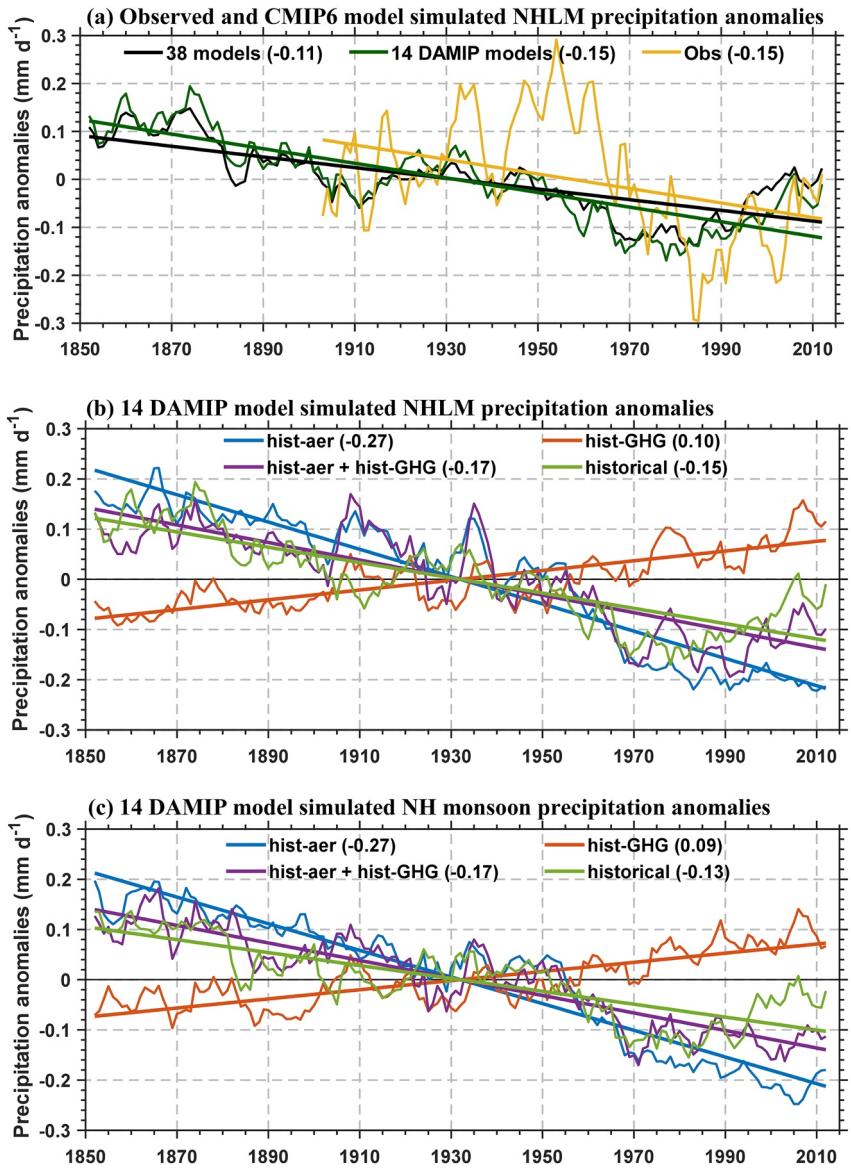

Figure 1. Anomalies and linear trends of Northern Hemisphere (NH) monsoon precipitation from observation and CMIP6 simulations. (a) Observed (yellow) and multi-model ensemble mean Northern Hemisphere land summer monsoon (NHLM) precipitation (mm d^{-1}) and trends (mm d^{-1} $cent^{-1}$) in 38 CMIP6 models (blue) and 14 DAMIP models (green). (b) The 14 DAMIP ensemble averaged NHLM precipitation in hist-aer (blue), hist-GHG (brown), historical (green) experiments, and the sum of hist-aer and hist-GHG experiment (hist-aer + hist-GHG, purple). (c) As (b), except for NH monsoon (the total of land and oceanic monsoon) precipitation. Observed precipitation anomaly is with respect to 1901–2014. Model simulated precipitation anomalies are with respect to 1850–2014. The thin lines denote the 5-year running mean and the thick lines denote the linear trends. All trends in the parentheses are significant at 95% level or higher.

significantly impact the NHLM precipitation, the decreasing NHLM since the 1950s is mainly attributed to the increased AA emission (Guo et al., 2013; Ha et al., 2020; Lau et al., 2006; Liepert et al., 2004; Polson et al., 2014; Song et al., 2014; Zhou et al., 2020). Polson et al. (2014) suggested that the decrease of NHLM precipitation since the 1950s can only be explained when including the influence of AA forcing, although the GHG forcing partially offsets its impact. Zhou et al. (2020) fully attributed the decline of NHLM to AA forcing and suggested that both the thermodynamic effect from the reduction of atmospheric humidity and the dynamic effect from the weakening of monsoon circulation are critical to the decline of monsoon precipitation since the 1950s. However, the declining trend is obtained over a relatively short period (Polson et al., 2014; Zhou et al., 2020). It may not well represent the impact of external forcing since the NHLM is significantly modulated by multi-decadal oscillation

19448007, 2022, 20, Downloaded from https://agupubs.onlinelibrary.wiley.com/doi/10.1029/2022GL100270 by CochraneChina, Wiley Online Library on [22/10/2022]. See the Terms and Conditions (https://onlinelibrary.wiley.com/terms-and-conditions) on Wiley Online Library for rules of use; OA articles are governed by the applicable Creative Commons License

(Wang et al., 2013, 2018). Therefore, a longer analysis period is more suitable for examining the impacts of external forcing. Moreover, the emission of both AA and GHG is along with the global industrialization (Figure S1 in Supporting Information S1); thus, their impacts on NHLM precipitation may exist since the 1850s. Until now, the paradox of centennial-scale NH monsoon precipitation drying and GMST increase is still unresolved, and the associated mechanism remains elusive.

Here we investigate the long-term change of NHLM precipitation and GMST using observed records and the simulations from Coupled Model intercomparison Project Phases 6 (CMIP6, Eyring et al., 2016) (Table S1 in Supporting Information S1). The Detection and Attribution MIP (DAMIP, Gillet et al., 2016) offers the single AA and GHG forcing experiments for understanding the impacts of individual forcing on NHLM precipitation. In DAMIP simulation, models suggest that the radiative forcing and the effects on GMST are more significant under GHG than AA forcing (Figure S1 and Table S2 in Supporting Information S1), while it is unknown the roles of the two forcings in affecting centennial-scale NH monsoon precipitation. In this work, we intend to address the following questions: (a) what is the relative role of AA and GHG forcing in the centennial-scale NHLM precipitation trend? (b) Why does the AA forcing dominate the declining NHLM precipitation, although AA's impacts on Earth system radiative forcing and GMST are less than GHG? (c) What mechanisms are responsible for the higher sensitivity of AA forcing on NH monsoon?

2. Data and Method

We used the surface temperature data from HadCRUT4 as observation (Morice et al., 2012). The arithmetic mean of three observed precipitation datasets is used to examine the long-term change in monsoon precipitation (IPCC, 2021; Monerie et al., 2022): (a) Version 7 of the Global Precipitation Climatology Centre covers 1901–2016 with a resolution of 0.5° × 0.5° (Schneider et al., 2014). (b) Version 4.04 of the Climate Research Unit covers 1901–2020 with a resolution of 0.5° × 0.5° (Harris et al., 2014). (c) Version 4.01 of the University of Delaware covers 1901–2017 with a resolution of 0.5° × 0.5° (Willmott et al., 2001). The 30-year climatology (1985–2014) of the Global Precipitation Climatology Project (Huffman et al., 2009) precipitation data is used to define the land and oceanic monsoon domain. It is the region where the precipitation difference between summer (May-September, MJJAS) and winter (November-March) exceeds 2.5 mm d^{-1}, and summer precipitation accounts for at least 55% of the annual total (Lee & Wang, 2014; Wang & Ding, 2006). This study focuses on the summer monsoon precipitation during MJJAS over the observed NH monsoon domain.

The historical simulation from 38 CMIP6 models is used to assess the model's ability to reproduce the observed long-term change of monsoon (Table S1 in Supporting Information S1). It is forced by the observed temporally evolving external forcings with the simulation period of 1850–2014 (Eyring et al., 2016). The roles of individual external forcings on monsoon precipitation are explored from DAMIP simulations: historical anthropogenic aerosol-only (hist-aer) and historical GHG-only (hist-GHG) experiments (Table S2 in Supporting Information S1). The hist-aer and hist-GHG experiments are designed as the historical experiment but forced by the AA only and well-mixed greenhouse gas only during 1850–2014, respectively (Gillet et al., 2016). The climate effects of AA and GHG forcing are evaluated by comparing the climatology mean of the most recent 30-year data (e.g., 1985–2014) with the corresponding pre-industrial simulation. The monthly mean variables used in this study include precipitation, evaporation, surface temperature, shortwave and longwave radiation, zonal wind, meridional wind, vertical pressure velocity, and specific humidity. The last four variables have 19 vertical layers extending from the surface to 1 hPa. All model data are re-gridded to a uniform resolution of 2° × 2° using bilinear interpolation.

To understand the mechanisms of changes in monsoon precipitation, a moisture budget analysis is used in this study. The Penman equation is used to quantify the surface potential evaporation over land (Howell & Evett, 2004; Penman, 1948). Details of the two methods are introduced in Text S1 in Supporting Information S1.

3. Results

3.1. Higher Efficiency of AA in Reducing Monsoon Precipitation

The emission of GHG and aerosol are continually increased since the industrial revolution. Global surface warming is accelerated caused by the increase of GHG emissions, albeit partially canceled by the cooling effect from

19448007, 2022, 20, Downloaded from https://agupubs.onlinelibrary.wiley.com/doi/10.1029/2022GL100270 by CochraneChina, Wiley Online Library on [22/10/2022]. See the Terms and Conditions (https://onlinelibrary.wiley.com/terms-and-conditions) on Wiley Online Library for rules of use; OA articles are governed by the applicable Creative Commons License

the aerosol (Figure S1 in Supporting Information S1). As opposed to the expectation that global warming would increase the precipitation, the observed NHLM had experienced significant drying since 1901 (Figure 1a). The NHLM rainfall exhibits a significant trend of ∼−0.15 mm d^{-1} per century ($p < 0.05$) since 1901. The historical experiment from 38 CMIP6 models well reproduces the decrease of monsoon rainfall, especially in the 14 DAMIP models (Figure 1a). The 14 DAMIP models' ensemble mean shows a significant decreasing trend of ∼−0.15 mm d^{-1} per century since 1850 for the NHLM rainfall (Figure 1a). The sum of AA-induced and GHG-induced NHLM precipitation changes has a decreasing linear trend of −0.17 mm d^{-1} per century since 1850, similar to the magnitude of the historical experiment (Figure 1b). It suggests the changes in NHLM precipitation during the historical period are roughly the linear summation of the impacts from AA and GHG forcing.

Once considering individual forcing separately, the single-forcing experiment suggests that the drying of NHLM is mainly attributable to the AA with only a limited contribution from the increase of GHG (Figure 1b). The AA could dry the monsoon with a significant trend of −0.27 mm d^{-1} per century ($p < 0.01$) over land. The GHG enhances the NHLM precipitation with a significant positive trend of +0.1 mm d^{-1} per century (Figure 1b), only partially offsetting the impact of AA. The monsoon precipitation shows coherent changes over land and ocean in hist-aer and hist-GHG experiments. The trends for land-only and the whole NH monsoon precipitation are both −0.27 mm d^{-1} per century under AA forcing, and the trends are similar (+0.1 vs. +0.09 mm d^{-1} per century) under GHG forcing (Figure 1c). This suggests that the AA dominates the drying of NH monsoon precipitation during the historical period.

The observed GMST shows a significant warming trend during the historical period, which is well reproduced by the CMIP6 models (Figure S1b in Supporting Information S1). This warming is dominated by the extensive GHG emission and partially mitigated by AA forcing. The 14 DAMIP models' ensemble mean shows the increase of GMST is 1.2 K by GHG, but only 0.6 K of decrease from AA forcing (i.e., the difference between 1985 and 2014 and the pre-industrial period), suggesting the higher efficiency of AA in changing NH monsoon precipitation in terms of per Kelvin of GMST change. The higher efficiency of AA is proved when scaled by GMST increase (Figure 2). It is also the case for the per unit of radiative forcing change since the AA-induced top-of-atmosphere radiative forcing intensity is only half that of GHG (Table S2 in Supporting Information S1).

Figure 2 quantitatively compared the monsoon precipitation sensitivity for different forcings. The observed NHLM monsoon precipitation shows a significant decrease of 0.16 mm d^{-1} K^{-1} since 1901. That means the NHLM precipitation is decreased by 2.8% for one Kelvin of GMST increase. The historical simulation shows the NHLM has a decrease rate of 0.13 mm d^{-1} K^{-1}, yielding the rate of −2.3% K^{-1}. It indicates that the CMIP6 model can well reproduce the negative monsoon precipitation sensitivity during the historical warming period (1850–2014). This contradicts the future projection result that gives a positive value of ∼2% K^{-1} (Cao et al., 2020; Wang et al., 2020). The individual forcing experiment shows that the historical GHG forced a rate of ∼2.1% K^{-1}; however, the AA causes a rate of ∼11% K^{-1}. The negative monsoon precipitation sensitivity (−2.3% K^{-1}) in the CMIP6 models is because the GHG dominates the GMST increase, but the AA dominates the precipitation reduction during the historical period (Figure 2a and Figure S1b in Supporting Information S1), yielding the higher precipitation sensitivity of AA. It exists over both the land and oceanic monsoon regions under AA forcing (Figure 2b).

According to the Clausius-Clapeyron relation, the atmospheric moisture can only enhance by ∼7% for a kelvin of global warming near present-day Earth surface temperature (Held & Soden, 2006). It limits the upper boundary of precipitation change from thermodynamic processes. The large ratio of precipitation change for one Kelvin of GMST change under AA forcing (∼11% K^{-1}) suggests that the dynamic effect and other factors can amplify the thermodynamic impact.

3.2. Evaporation and Monsoon Circulation Contributions to the Higher Precipitation Sensitivity

The precipitation and GMST changes between the recent 30-year climatology (1985–2014) of hist-aer (hist-GHG) experiment and the pre-industrial simulation are used to diagnose the factors that cause the higher sensitivity of monsoon precipitation under AA forcing. We compared the climate impacts of AA and GHG on monsoon precipitation changes and their associated factors as shown in Equation 3 of Text S1 in Supporting Information S1 (Figure 3). When forced by GHG, the increase of NHLM precipitation is dominated by the enhancement of atmospheric moisture ($\langle \overline{\omega}\partial_p q' \rangle$) and compensated by the weakening of monsoon circulation ($\langle \omega' \partial_p \overline{q} \rangle$)

19448007, 2022, 20, Downloaded from https://agupubs.onlinelibrary.wiley.com/doi/10.1029/2022GL100270 by CochraneChina, Wiley Online Library on [22/10/2022]. See the Terms and Conditions (https://onlinelibrary.wiley.com/terms-and-conditions) on Wiley Online Library for rules of use; OA articles are governed by the applicable Creative Commons License

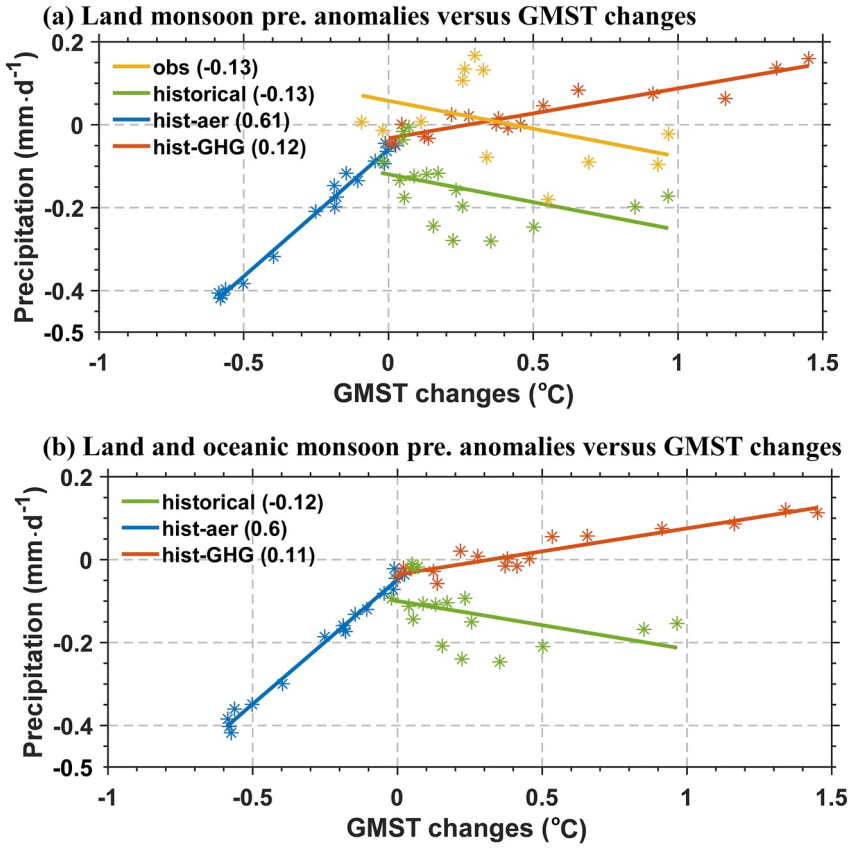

Figure 2. Scatter plots of decadal means of the (a) Northern Hemisphere land summer monsoon (NHLM) precipitation (mm d^{-1}) anomalies and (b) Northern Hemisphere (NH) monsoon (the total of land and ocean) precipitation anomalies versus global mean surface temperature (°C) changes. The reference period for observation is 1901–1930. The reference for simulation is the corresponding pre-industrial experiment. The numbers in the parentheses are slopes, which indicate the monsoon precipitation sensitives (mm d^{-1} K^{-1}) under difference forcing.

(Figure 3a). Thus, a moderate change in NHLM is seen under GHG forcing. However, the situation is different under AA forcing: the reduction of NHLM precipitation is caused by the decreased evaporation, reduced atmospheric moisture content, and weakened ascending motion over the monsoon region (Figure 3). It suggests that the reduced evaporation and vertical moisture advection due to the weakening of monsoon circulation primarily decreased precipitation, and the reduced moisture content enhanced the precipitation reduction. Thus, the monsoon precipitation change is larger in the hist-aer experiment than in the hist-GHG experiment, leading to the dominant role of AA on NH monsoon change during the historical period.

When scaling the precipitation change and its components by the corresponding GMST change (Figure 3b), it finds that the higher sensitivity of evaporation and monsoon circulation responses are both critical to the higher precipitation efficiency of AA. Dramatic differences exist in evaporation terms and dynamic terms, although the thermodynamic terms are comparable under the two forcings (Figure 3b). Thus, it is crucial to reveal the mechanisms driving the higher sensitivity of evaporation and monsoon circulation responses to AA.

3.3. Surface Radiation Drives Higher Precipitation Sensitivity Under AA Forcing

How can the AA cause the larger changes in surface evaporation and monsoon circulation for a unit of GMST change compared to GHG? In the high precipitated monsoon region, the surface evaporation is more constrained by the available energy for evaporation and minorly constrained by water availability (Liepert et al., 2004; Roderick et al., 2014). Therefore, the Penman equation is used to quantify the surface potential evaporation (Text S1 in Supporting Information S1). The change of evaporation is dominated by the net surface irradiance since

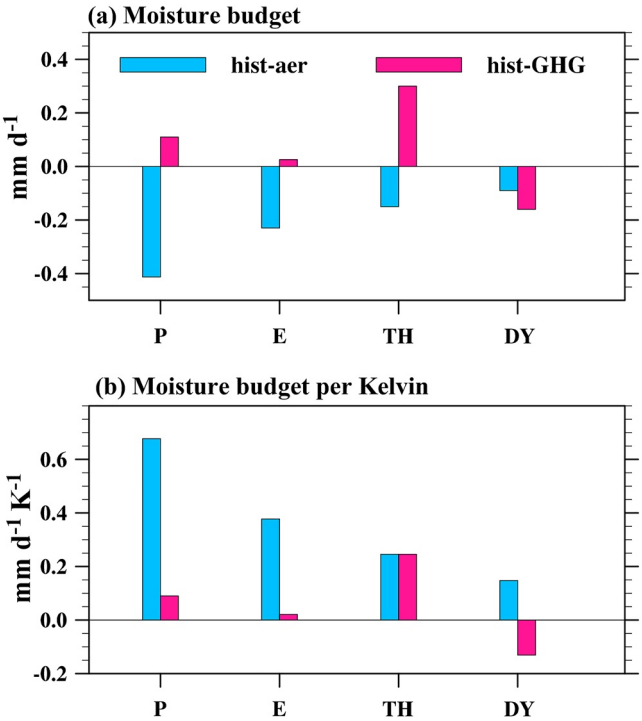

Figure 3. The moisture budget analysis shows the key factors to Northern Hemisphere land summer monsoon (NHLM) precipitation change. (a) Moisture budget analysis for precipitation change (mm d^{-1}), (b) is (a) scaled by the global mean surface temperature (GMST) changes with the unit of mm d^{-1} K^{-1}. P indicates precipitation, and E indicates evaporation. TH and DY represent the thermodynamic and dynamic component of the vertical moisture convergence, respectively.

other parameters are either constant or have no apparent changes due to the relatively small surface temperature change (~1 K) to historical GHG and aerosol forcing (Equation 4 of Text S1 in Supporting information S1).

Figures 4a and 4b illustrate the changes in net surface irradiance scaled by GMST change from hist-aer and hist-GHG experiments, respectively. For one Kelvin of GMST increase, the response of surface irradiance is more prominent under AA forcing than GHG forcing, suggesting the AA forcing is more effective in modulating the surface energy budget (Figures 4a and 4b). Physically, the aerosol-radiation and aerosol-cloud interactions can significantly change the downward solar radiation, thus modulating the net surface irradiance. During the historical period, the AA emission is more prominent in the industrial regions, where primarily located in the NH monsoon area. Consistent with the global distribution of AA optical depth change, the response of downward shortwave radiation dominates the net surface irradiance change (Figure S2 in Supporting Information S1). It shows apparent heterogeneous features with a larger response over global land than the ocean and a larger response over the NH than in the Southern Hemisphere (SH) (Figure 4a). Locally, the net surface irradiance change is more sensitive over the NH monsoon region (Figure 4a). Over this region, the change is 11.8 W m^{-2} K^{-1} under AA forcing, four times larger than that under GHG forcing with the value of 2.1 W m^{-2} K^{-1}. Therefore, the AA effectively alters the net surface radiation availability for surface evaporation, thus significantly modulating surface evaporation. On the other hand, the plant physiology response to the increase of CO_2 could mitigate the increase of evaporation under GHG forcing (Swann et al., 2016). In sum, the above-mentioned processes all contribute to the higher sensitivity of monsoon precipitation change to AA (Figure 3b).

Monsoon circulation is also an effective factor in forming higher precipitation sensitivity to AA than GHG. Figure 4c shows the pattern of surface temperature change scaled by the GMST change due to the AA forcing. The scaled surface temperature is characterized by the NH-warmer-than-SH and land-warmer-than-ocean pattern, leading to the enhancement of inter-hemispheric temperature difference (ITD) and land-ocean thermal contrast (LOTC) during the boreal summer (Figure 4c). That means the increase of AA, as in the historical period, could decrease the ITD and LOTC, but the reduction of AA could enhance the ITD and LOTC (as in Figure 4c). The anomalous surface temperature alters the sea level pressure, leading to the high-pressure anomaly over the SH and the low-pressure anomaly over the NH. It drives the low-level circulation, thus enhancing the northward across-equatorial flow, especially over the monsoon region (Figure 4e). The warmer land benefits the moisture convergence over the monsoon region, thus enhancing the mid-troposphere ascending motion (Figure 4g), leading to amplified precipitation response under AA forcing (Figure 4e). The strong dynamic effect from northward cross-equatorial flow and circulation convergence over land could overwhelm the enhanced atmospheric static stability due to the increase of GMST (Figure S3a in Supporting Information S1). Thus, the net effect shows the enhanced dynamic effect under the AA reduction-induced global warming. In other words, the increase of AA emission during the historical period weakens the dynamic effect that suppresses monsoon precipitation.

In contrast, the NH-warmer-than-SH and the land-warmer-than-ocean surface temperature responses are much weaker from GHG than AA forcing (Figures 4c and 4d). The marginally enlarged ITD and LOTC have little impact on monsoon circulation (Figure 4f). It is overwhelmed by the increased atmospheric static stability (Figure S3b in Supporting Information S1), leading to the weakened ascending motion over the monsoon region (Figure 4h). Therefore, the dynamic effect has a negative effect on precipitation change, which partially cancels the thermodynamic effect, yielding a moderate precipitation response under GHG forcing (Figure 3).

Figure 5 quantitatively compared the thermodynamic indices and their associated monsoon circulation indices based on Figure 4. Note that all indices are scaled by the GMST change from hist-aer and hist-GHG experiments, respectively. As suggested by previous studies, two thermal indices are used to represent the heterogeneous global

19448007, 2022, 20, Downloaded from https://agupubs.onlinelibrary.wiley.com/doi/10.1029/2022GL100270 by CochraneChina, Wiley Online Library on [22/10/2022]. See the Terms and Conditions (https://onlinelibrary.wiley.com/terms-and-conditions) on Wiley Online Library for rules of use; OA articles are governed by the applicable Creative Commons License

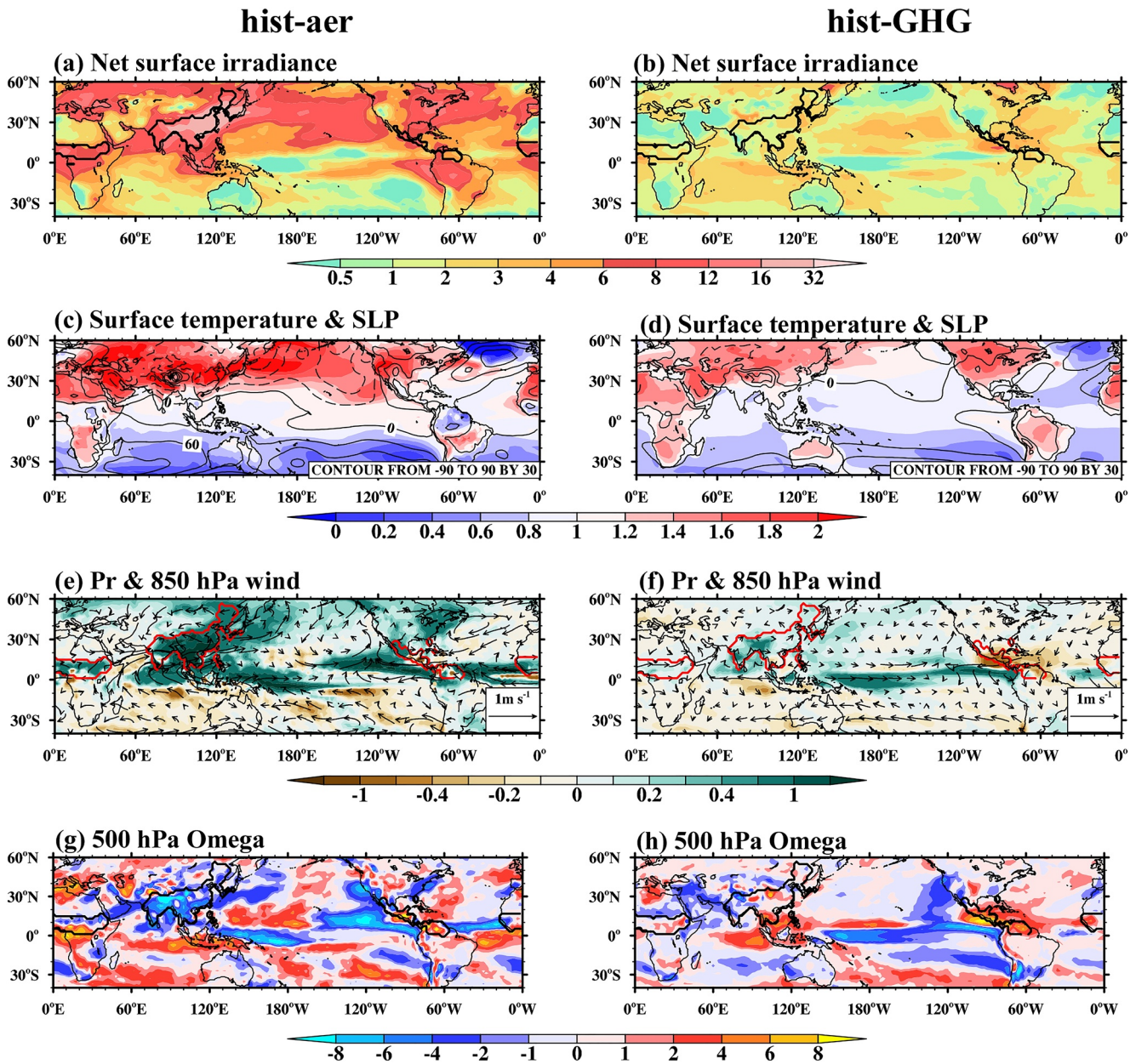

Figure 4. Comparison of atmospheric variables responds to anthropogenic aerosol (AA) (left) and greenhouse gases (GHG) (right) forcing. All changes are scaled by the corresponding global mean surface temperature (GMST) changes from hist-aer and hist-GHG experiments. (a and b) for net surface irradiance (W m^{-2} K^{-1}). (c and d) for surface temperature (shading, K K^{-1}) and sea level pressure (contour, Pa K^{-1}). (e and f) for precipitation (mm d^{-1} K^{-1}) and 850 hPa circulation (m s^{-1} K^{-1}). (g) and (h) for vertical pressure velocity (hPa d^{-1} K^{-1}) at 500 hPa. The black and red lines outline the Northern Hemisphere (NH) land monsoon region.

warming that has dominant effects on monsoon circulation changes (Cao et al., 2020; Wang et al., 2013, 2020). The ITD index is defined as the surface temperature difference between the NH [0–40°N, 0°–360°] and SH [0°–60°S, 0°–360°]. The LOTC index is defined as the temperature difference between NH land [0°–60°N, 0°–360°] and global ocean [60°S–60°N, 0°–360°]. The monsoon circulation indices describe how the atmospheric circulation change could affect the moisture transport and precipitation intensity. The low-level cross-equatorial flow from the SH to NH (EQ_V index) is defined as the meridional wind averaged over [5°S–10°N, 0°–360°] at 925 hPa. And the zonal wind shear between 200 and 850 hPa over the band of [0°–20°N, 120°W–120°E] is defined as the U_shear index (Wang et al., 2013). Once one Kelvin of GMST warming is caused by AA reduction, the ITD would enhance by ∼1 K, suggesting the warmer-NH and cooler-SH is more significant during the boreal summer (Figure 5a). Thus, it could enhance the low-troposphere northward moisture transport through the strengthened

19448007, 2022, 20, Downloaded from https://agupubs.onlinelibrary.wiley.com/doi/10.1029/2022GL100270 by CochraneChina, Wiley Online Library on [22/10/2022]. See the Terms and Conditions (https://onlinelibrary.wiley.com/terms-and-conditions) on Wiley Online Library for rules of use; OA articles are governed by the applicable Creative Commons License

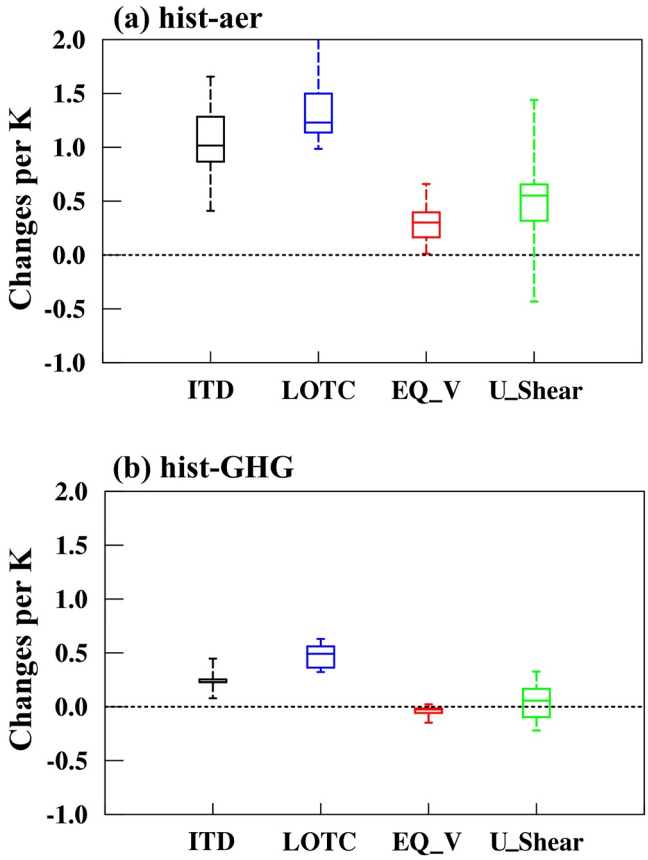

Figure 5. More effective thermodynamic and dynamic indices responses under anthropogenic aerosol (AA) forcing than greenhouse gases (GHG) forcing. (a) Indices changes under 1 K of global mean surface temperature (GMST) warming due to AA forcing. (b) Indices changes under 1 K of GMST change due to GHG forcing. Indices are interhemispheric temperature differences (ITD, K K^{-1}), land-ocean temperature contrast (LOTC, K K^{-1}), cross-equatorial meridional winds (EQ_V, m s^{-1} K^{-1}) at 925 hPa, and zonal wind shear between 850 hPa and 200 hPa (U_shear, m s^{-1} K^{-1}). Whiskers, boxes, and the bars inside the boxes represent the 10th–90th percentiles, quartile range, and median, respectively.

cross-equatorial flow (EQ_V, Figure 5a). On the other hand, the reduction of AA enhances the LOTC. Along with the enhanced ITD, it accelerates the zonal wind shear over the monsoon region (Figure 5a), thus strengthening the moisture convergence (Figures 3b and 4e). Therefore, when reduces the AA emission, the dynamic effect from the enhanced monsoon circulation amplifies the impacts of thermodynamic effect and evaporation, leading to the more efficient impact of AA on NH monsoon precipitation change. The opposite is true for the increase of AA during the historical period, causing the amplified reduction of monsoon precipitation and high monsoon precipitation sensitivity (Figure 3).

However, the thermal contrast indices from GHG forcing are considerably smaller than that from AA forcing (Figure 4d), indicating that the GHG-induced global warming shows less interhemispheric and land-sea contrast pattern. It is one of the reasons that the circulation indices are nearly unchanged in hist-GHG experiment (Figure 5b). On the other hand, the GHG-induced El-Nino-like sea surface temperature warming over the Pacific Ocean can weaken the northward cross-equatorial flow and zonal wind shear over the eastern Pacific-north American monsoon region (Figures 4f and 5b). Therefore, the enhanced atmospheric static stability due to the top-heavy warming under GHG forcing dominates the weakening of the dynamic effect (Figure 3, Figure S3b in Supporting Information S1).

4. Summary

Since 1901, the GMST has increased by ~1°C (IPCC, 2021). In common sense, global warming would increase monsoon precipitation. However, observation shows a drying NHLM since 1901. The CMIP6 historical simulation can well reproduce the decrease of observed NHLM precipitation since the industrial revolution forced by external forcings. The CMIP6 model result further shows the drying is coherent over land and oceanic monsoon regions, consistent with the coherent variation of land and ocean monsoon precipitation under anthropogenic forcing in most prior studies (Ha et al., 2020; Lee & Wang, 2014). The concurrent increase in AA and GHG emissions are the two major drivers. However, they show distinct efficiency in changing the NH monsoon precipitation. The AA dominates the NH monsoon precipitation change but only has a minor role in the Earth's surface temperature. In contrast, the GHG mainly controls the Earth's surface warming but has a minor role in changing monsoon precipitation. Thus, the AA is more efficient in changing NH monsoon precipitation for a unit GMST change.

Moisture conservation diagnosis suggests that the surface evaporation and vertical moisture convergence from monsoon circulation are the major factors in determining the higher efficiency of AA. The intensive AA emission is concentrated over the populated monsoon region, where industrialization is rapid. The reduction of downward shortwave radiation due to aerosol-radiation and aerosol-cloud interactions weakens the net solar irradiance for evaporation. Meanwhile, it reduces the ITD and LOTC, thus significantly weakening the monsoon circulation. Both of these two processes are much more effective under the AA forcing than the GHG forcing, resulting in the higher efficiency of the AA in changing NH monsoon precipitation. Thus, the AA dominates the NH monsoon precipitation reduction, albeit its impact on GMST is small. Alternatively, GHG dominates global warming but has a minor effect on NH monsoon precipitation change. Our result indicates the future reduction of AA and increase of GHG emission would rapidly recover the NH monsoon precipitation due to their in-phase impact.

Conflict of Interest

The authors declare no conflicts of interest relevant to this study.

19448007, 2022, 20, Downloaded from https://agupubs.onlinelibrary.wiley.com/doi/10.1029/2022GL100270 by CochraneChina, Wiley Online Library on [22/10/2022]. See the Terms and Conditions (https://onlinelibrary.wiley.com/terms-and-conditions) on Wiley Online Library for rules of use; OA articles are governed by the applicable Creative Commons License

Data Availability Statement

The CMIP6 models used in this study can be found in Table S1 in Supporting Information S1. The model data is available from: https://esgf-node.llnl.gov/projects/cmip6/. The authors acknowledge the World Climate Research Programme's Working Group on Coupled Modelling, which is responsible for CMIP.

Acknowledgments
Jian Cao acknowledges the support from the Natural Science Foundation of China of Jiangsu Province (BK20220108) and Natural Science Foundation of China (42005017, 41730961). Haikun Zhao acknowledges the support from the Natural Science Foundation of China (41922033, 42192551). Xiaowei Zhu acknowledges the support from Key research and development program of Ningxia (2022BEG03058). The authors acknowledge the computer resources at the NUIST High Performance Computer Center. This is ESMC publication NO. 391, IPRC publication NO. 1579, and SOEST publication NO. 11582.

References

Cao, J., Wang, B., & Ma, L. (2019). Attribution of global monsoon response to the last glacial maximum forcings. *Journal of Climate*, *32*(19), 6589–6605. https://doi.org/10.1175/JCLI-D-18-0871.1

Cao, J., Wang, B., Wang, B., Zhao, H., Wang, C., & Han, Y. (2020). Sources of the intermodel spread in projected global monsoon hydrological sensitivity. *Geophysical Research Letters*, *47*(18), e2020GL089560. https://doi.org/10.1029/2020GL089560

Cao, J., & Zhao, H. (2020). Distinct response of Northern Hemisphere land monsoon precipitation to transient and stabilized warming scenarios. *Advances in Climate Change*, *11*(3), 161–171. https://doi.org/10.1016/j.accre.2020.09.007

Chadwick, R., Boutle, I., & Martin, G. (2013). Spatial patterns of precipitation change in CMIP5: Why the rich do not get richer in the tropics. *Journal of Climate*, *26*(11), 3803–3822. https://doi.org/10.1175/JCLI-D-12-00543.1

Eyring, V., Bony, S., Meehl, G. A., Senior, C. A., Stevens, B., Stouffer, R. J., & Taylor, K. E. (2016). Overview of the coupled model intercomparison project phase 6 (CMIP6) experimental design and organization. *Geoscientific Model Development*, *9*(5), 1937–1958. https://doi.org/10.5194/gmd-9-1937-2016

Gillett, N. P., Shiogama, H., Funke, B., Hegerl, G., Knutti, R., Matthes, K., et al. (2016). The detection and attribution model intercomparison project (DAMIP v1.0) contribution to CMIP6. *Geoscientific Model Development*, *9*(10), 3685–3697. https://doi.org/10.5194/gmd-9-3685-2016

Guo, L., Highwood, E. J., Shaffrey, L. C., & Turner, A. G. (2013). The effect of regional changes in anthropogenic aerosols on rainfall of the East Asian Summer Monsoon. *Atmospheric Chemistry and Physics*, *13*(3), 1521–1534. https://doi.org/10.5194/acp-13-1521-2013

Ha, K. J., Kim, B. H., Chung, E. S., Chan, J. C. L., & Chang, C. P. (2020). Major factors of global and regional monsoon rainfall changes: Natural versus anthropogenic forcing. *Environmental Research Letters*, *15*(3), 034055. https://doi.org/10.1088/1748-9326/ab7767

Harris, I., Jones, P. D., Osborn, T. J., & Lister, D. H. (2014). Updated high-resolution grids of monthly climatic observations-The CRU TS3.10 dataset. *International Journal of Climatology*, *34*(3), 623–642. https://doi.org/10.1002/joc.3711

Held, I. M., & Soden, B. J. (2006). Robust responses of the hydrological cycle to global warming. *Journal of Climate*, *19*(21), 5686–5699. https://doi.org/10.1175/JCLI3990.1

Herman, R., Giannini, A., Biasutti, M., & Kushnir, Y. (2020). The effects of anthropogenic and volcanic aerosols and greenhouse gases on twentieth century Sahel precipitation. *Scientific Reports*, *10*(1), 12203. https://doi.org/10.1038/s41598-020-68356-w

Howell, T., & Evett, S. (2004). *The Penman-Monteith method*. USDA-Agricultural Research Service Conservation & Production Research Laboratory.

Hsu, P. C., Li, T., Murakami, H., & Kitoh, A. (2013). Future change of the global monsoon revealed from 19 CMIP5 models. *Journal of Geophysical Research: Atmospheres*, *118*(3), 1247–1260. https://doi.org/10.1002/jgrd.50145

Huffman, G. J., Adler, R. F., Bolvin, D. T., & Gu, G. (2009). Improving the global precipitation record: GPCP version 2.1. *Geophysical Research Letters*, *36*(17), L17808. https://doi.org/10.1029/2009GL040000

IPCC. (2021). Climate change 2021: The physical science basis. In V. Masson-Delmotte, P. Zhai, A. Pirani, S. L. Connors, C. Péan, S. Berger, et al. (Eds.), *Contribution of working group I to the sixth assessment report of the intergovernmental panel on climate change*. Cambridge University Press. https://doi.org/10.1017/9781009157896

Jin, C., Wang, B., & Liu, J. (2020). Future changes and controlling factors of the eight regional monsoons projected by CMIP6 models. *Journal of Climate*, *33*(21), 9037–9326. https://doi.org/10.1175/JCLI-D-20-0236.1

Kitoh, A., Endo, H., Krishna, K., Cavalcanti, I., Goswami, P., & Zhou, T. (2013). Monsoons in a changing world: A regional perspective in a global context. *Journal of Geophysical Research: Atmospheres*, *118*(8), 3053–3065. https://doi.org/10.1002/jgrd.50258

Lau, K. M., Kim, M. K., & Kim, K. M. (2006). Asian summer monsoon anomalies induced by aerosol direct forcing: The role of the Tibetan Plateau. *Climate Dynamics*, *26*(7–8), 855–864. https://doi.org/10.1007/s00382-006-0114-z

Lee, J. Y., & Wang, B. (2014). Future change of global monsoon in the CMIP5. *Climate Dynamics*, *42*(1–2), 101–119. https://doi.org/10.1007/s00382-012-1564-0

Liepert, B. G., Feichter, J., Lohmann, U., & Roeckner, E. (2004). Can aerosols spin down the water cycle in a warmer and moister world? *Geophysical Research Letters*, *31*(6), L06207. https://doi.org/10.1029/2003GL019060

Monerie, P. A., Wilcox, L., & Turner, A. (2022). Effects of anthropogenic aerosol and greenhouse gas emissions on northern hemisphere monsoon precipitation: Mechanisms and uncertainty. *Journal of Climate*, *35*(8), 2305–2326. https://doi.org/10.1175/JCLI-D-21-0412.1

Moon, S., & Ha, K. J. (2020). Future changes in monsoon duration and precipitation using CMIP6. *NPJ Climate and Atmospheric Science*, *3*(1), 45. https://doi.org/10.1038/s41612-020-00151-w

Morice, C. P., Kennedy, J. J., Rayner, N. A., & Jones, P. D. (2012). Quantifying uncertainties in global and regional temperature change using an ensemble of observational estimates: The HadCRUT4 data set. *Journal of Geophysical Research*, *117*(D8), D08101. https://doi.org/10.1029/2011JD017187

Penman, H. L. (1948). Natural evaporation from open water, hare soil and grass. *Proceedings of the royal society of London. Series A. Mathematical and physical sciences*, *193*, 120–145. https://doi.org/10.1098/rspa.1948.0037

Polson, D., Bollasina, M., Hegerl, G. C., & Wilcox, L. J. (2014). Decreased monsoon precipitation in the Northern Hemisphere due to anthropogenic aerosols. *Geophysical Research Letters*, *41*(16), 6023–6029. https://doi.org/10.1002/2014GL060811

Roderick, M. L., Sun, F., Lim, W. H., & Farquhar, G. D. (2014). A general framework for understanding the response of the water cycle to global warming over land and ocean. *Hydrology and Earth System Sciences*, *18*(5), 1575–1589. https://doi.org/10.5194/hess-18-1575-2014

Schneider, U., Becker, A., Finger, P., Meyer-Christoffer, A., Ziese, M., & Rudolf, B. (2014). GPCC's new land surface precipitation climatology based on quality-controlled in situ data and its role in quantifying the global water cycle. *Theoretical and Applied Climatology*, *115*(1–2), 15–40. https://doi.org/10.1007/s00704-013-0860-x

Song, F., Zhou, T., & Qian, Y. (2014). Responses of East Asian summer monsoon to natural and anthropogenic forcings in the 17 latest CMIP5 models. *Geophysical Research Letters*, *41*(2), 596–603. https://doi.org/10.1002/2013GL058705

Swann, A., Hoffman, F., Koven, C. D., & Randerson, J. T. (2016). Plant responses to increasing CO_2 reduce estimates of climate impacts on drought severity. *Proceedings of the National Academy of Sciences*, *36*, 10019–10024. https://doi.org/10.1073/pnas.1604581113

19448007, 2022, 20, Downloaded from https://agupubs.onlinelibrary.wiley.com/doi/10.1029/2022GL100270 by CochraneChina, Wiley Online Library on [22/10/2022]. See the Terms and Conditions (https://onlinelibrary.wiley.com/terms-and-conditions) on Wiley Online Library for rules of use; OA articles are governed by the applicable Creative Commons License

Vicente-Serrano, S., Garcia-Herrera, R., Pena-Angulo, D., Tomas-Burguera, M., Dominguez-Castro, F., Noguera, I., et al. (2021). Do CMIP models capture the long-term observed annual precipitation trends? *Climate Dynamics*, *58*(9–10), 2825–2842. https://doi.org/10.1007/s00382-021-06034-x

Wang, B., Cane, M. A., Liu, J., Webster, P. J., Xiang, B., Kim, H.-M., et al. (2018). Toward predicting changes in the land monsoon rainfall a decade in advance. *Journal of Climate*, *31*(7), 2699–2714. https://doi.org/10.1175/JCLI-D-17-0521.1

Wang, B., & Ding, Q. (2006). Changes in global monsoon precipitation over the past 56 years. *Geophysical Research Letters*, *33*(6), 1–4. https://doi.org/10.1029/2005GL025347

Wang, B., Jin, C., & Liu, J. (2020). Understanding future change of global monsoons projected by CMIP6 models. *Journal of Climate*, *33*(15), 6471–6489. https://doi.org/10.1175/JCLI-D-19-0993.1

Wang, B., Liu, J., Kim, H. J., Webster, P. J., Yim, S. Y., & Xiang, B. (2013). Northern Hemisphere summer monsoon intensified by mega-El Niño/southern oscillation and Atlantic multi-decadal oscillation. *Proceedings of the National Academy of Sciences*, *110*(14), 5347–5352. https://doi.org/10.1073/pnas.1219405110

Willmott, C. J., Matsuura, K., & Legates, D. R. (2001). *Terrestrial air temperature and precipitation: Monthly and annual time series (1950–1999), version 1*. Center for Climatic Research. Retrieved from http://climate.geog.udel.edu/~climate/html_pages/README.ghcn_ts2.html

Zhang, L., & Zhou, T. (2011). An assessment of monsoon precipitation changes during 1901–2001. *Climate Dynamics*, *37*(1–2), 279–296. https://doi.org/10.1007/s00382-011-0993-5

Zhou, T., Yu, R., Li, H., & Wang, B. (2008). Ocean forcing to changes in global monsoon precipitation over the recent half-century. *Journal of Climate*, *21*(15), 3833–3852. https://doi.org/10.1175/2008JCLI2067.1

Zhou, T., Zhang, W., Zhang, L., Zhang, X., Qian, Y., Peng, D., et al. (2020). The dynamic and thermodynamic processes dominating the reduction of global land monsoon precipitation driven by anthropogenic aerosols emission. *Science China Earth Sciences*, *63*(7), 919–933. https://doi.org/10.1007/s11430-019-9613-9

19448007, 2022, 20, Downloaded from https://agupubs.onlinelibrary.wiley.com/doi/10.1029/2022GL100270 by CochraneChina, Wiley Online Library on [22/10/2022]. See the Terms and Conditions (https://onlinelibrary.wiley.com/terms-and-conditions) on Wiley Online Library for rules of use; OA articles are governed by the applicable Creative Commons License